Inorg. Chem. **2006**, *45*, 3478–3480

New Cuprates Featuring Ladderlike Periodic Arrays of $[Cu_3O_8]^{10-}$ Trimeric Magnetic Nanostructures

Xunhua Mo,[†] Kristen M. S. Etheredge,[‡] Shiou-Jyh Hwu,*[,†] and Qun Huang[†]

Department of Chemistry, Clemson University, Clemson, South Carolina 29634-0973, and Department of Chemistry, Rice University, Houston, Texas 77251

Received February 20, 2006

A new family of cuprates, $Li_2Cu_3(SiO_3)_4$ (**1**) and $Na_2Cu_3(GeO_3)_4$ (**2**), was isolated in molten salt media. The extended lattices contain ladderlike periodic arrays of $[Cu_3O_8]^{10-}$ magnetic nanostructures. Magnetic properties of the $Na_2Cu_3Ge_{4-x}Si_xO_{12}$ series, where $x = 0$, 0.86, and 1.72, were systematically studied. The geometrically induced magnetic couplings are tunable upon cation substitution.

Extended solids consisting of periodic arrays of nanostructures are attractive because of their simplified structures and molecule-like (quantized) physical properties. These have been exemplified by a family of newly developed magnetic insulators in which the magnetic nanostructures made of transition-metal (TM) oxides are imbedded in a closed-shell, nonmagnetic oxy anion matrix, which include silicates, phosphates, and arsenates.[1] Compounds containing structurally confined copper oxide nanostructures have been perceived as a model for spin−spin and spin−lattice correlation studies,[2,3] leading to a fundamental understanding of magnetic phenomena associated with cuprate superconductors. Also, TM oxide containing oxy compounds of this kind have been the recent subject of many studies[3a,4] complementary to the so-called single-molecule magnets[5] and molecular nanomagnets,[6] which exhibit nanometer-sized single-domain magnetic particles with high-spin ground states. In this Communication, we report a fascinating family of cuprates, $Li_2Cu_3(SiO_3)_4$ (**1**) and $Na_2Cu_3(GeO_3)_4$ (**2**), that exhibit ladderlike periodic arrays of $[Cu_3O_8]^{10-}$ nanostructures. This spin trimer system possesses by far the closest molecule-like multinuclear nanostructures that we have observed, judging from their comparable magnetic behaviors with those of a reported Cu^{II} trimer complex.[7]

1 and **2** form platelike blue crystals grown in molten salt media.[8] **1** was serendipitously discovered in a reaction as a result of accidental incorporation of the silicate anion from the employed quartz ampule.[9] Attempts to produce **1** in high yield failed but were successful in isolating its Na/Ge analogue, **2**. Discussion of the structure and properties of this novel series of cuprates is, therefore, based on **2** and its Si-doped $Na_2Cu_3Ge_{4-x}Si_xO_{12}$ ($x = 0.86$ and 1.72) analogues.[10] It is noted that an isomorphous phase, $Na_2Cu_3Si_4O_{12}$,

* To whom correspondence should be addressed. E-mail: shwu@clemson.edu.

[†] Clemson University.

[‡] Rice University.

(1) Hwu, S.-J. *Chem. Mater.* **1998**, *10*, 2846−2859.

(2) For example, see the following. (a) $A_3Cu_3(PO_4)_3$ (A = Ca, Sr, Pb): Matsuda, M.; Kakurai, K.; Belik, A. A.; Azuma, M.; Takano, M.; Fujita, M. *Phys. Rev. B* **2005**, *71*, 144411/1−144411/5. (b) β-$Cu_3V_2O_8$: Rogado, N.; Haas, M. K.; Lawes, G.; Huse, D. A.; Ramirez, A. P.; Cava, R. J. *J. Phys.: Condens. Matter* **2003**, *15*, 907−914. (c) $BaCu_2(Si_{1-x}Ge_x)_2O_7$: Yamada, T.; Hiroi, Z.; Takano, M. *J. Solid State Chem.* **2001**, *156*, 101−109. (d) $CuGeO_3$: Mizuno, Y.; Tohyama, T.; Maekawa, S.; Osafune, T.; Motoyama, N.; Eisaki, H.; Uchida, S. *Phys. Rev.* **1998**, *B57*, 5326−5335.

(3) (a) $Cs_2Cu_3P_4O_{14}$: Ranmohotti, K. G. S.; Mo, X.; Smith, M. K.; Hwu, S.-J. *Inorg. Chem.* **2005**, in press. (b) $NaCuAsO_4$: Ultagay-Kartin, M.; Hwu, S.-J.; Clayhold, J. A. *Inorg. Chem.* **2003**, *42*, 2405−2409. (c) $Na_5ACu_4(AsO_4)_4Cl_2$ (A = Rb, Cs): Hwu, S.-J.; Ultagay-Kartin, M.; Clayhold, J. A.; Mackay, R.; Wardojo, T. A.; O'Connor, C. J.; Krawiec, M. *J. Am. Chem. Soc.* **2002**, *124*, 12404−12405.

(4) (a) Queen, W.; Hwu, S.-J. *Chem. Commun.* **2005**, submitted for publication. (b) Ulutagay-Kartin, M.; Etheredge, K. M. S. G.; Schimek, G. L.; Hwu, S.-J. *J. Alloys Compd.* **2002**, *338*, 80−86.

(5) For example, see: (a) Lecren, L.; Wernsdorfer, W.; Li, Y.-G.; Roubeau, O.; Miyasaka, H.; Clerac, R. *J. Am. Chem. Soc.* **2005**, *127* (32), 11311−11317. (b) Rajaraman, G.; Murugesu, M.; Sañudo, E. C.; Soler, M.; Wernsdorfer, M.; Helliwell, M.; Muryn, C.; Raftery, J.; Teat, S. J.; Christou, G.; Brechin, E. K. *J. Am. Chem. Soc.* **2004**, *126*, 15445−15447. (c) Wernsdorfera, W.; Aliaga-Alcaldeb, N.; Tirona, R.; Hendricksonc, D. N.; Christou, G. *J. Magn. Magn. Mater.* **2004**, *272−276*, 1037−1041. (d) Murugesu, M.; Raftery, J.; Wernsdorfer, W.; Christou, G.; Brechin, E. K. *Inorg. Chem.* **2004**, *43*, 4203−4209 and references cited therein. (e) Gatteschi, D.; Caneschi, A.; Pardi, L.; Sessoli, R. *Science* **1994**, *265*, 1054−1058.

(6) Thompson, L. K.; Waldmann, O.; Xu, Z. *Coord. Chem. Rev.* **2005**, *249*, 2677−2690.

(7) Pashchenko, V.; Brendel, B.; Wolf, B.; Lang, M.; Lyssenko, K.; Shchegolikhina, O.; Molodtsova, Y.; Zherlitsyna, L.; Auner, N.; Schütz, F.; Kollar, M.; Kopietz, P.; Harrison, N. *Eur. J. Inorg. Chem.* **2005**, 4617−4625.

(8) Crystals of **2**, for example, were grown by employing a eutectic CsCl/NaCl flux in a Al_2O_3 crucible sealed in a fused silica ampule under vacuum. Aldrich Na_2O (1 mmol, 85%), CuO (3 mmol, 99.99%), and GeO_2 (4 mmol, 99.99%) were mixed and ground with flux (1:3 by weight) in a nitrogen-blanketed drybox. The mixture was heated to 650 °C and isothermed for 3 days, followed by slow cooling to 300 °C at 6 °C/h and then furnace cooling to room temperature. Crystals (90% based on CuO) were retrieved by washing off the salt with deionized water.

(9) Etheredge, K. M. S. Ph.D. Dissertation, Rice University, Houston, TX, 1996.

(10) Mo, X. Ph.D. Dissertation, Clemson University, Clemson, SC, 2004.

10.1021/ic060292q CCC: $33.50
Published on Web 03/28/2006

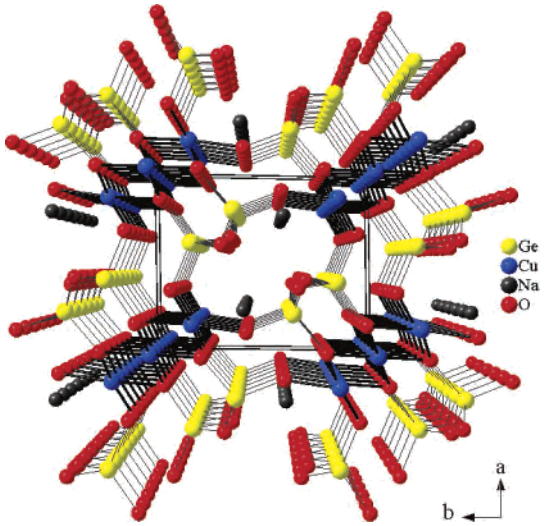

Figure 1. Perspective view of **2** showing channels.

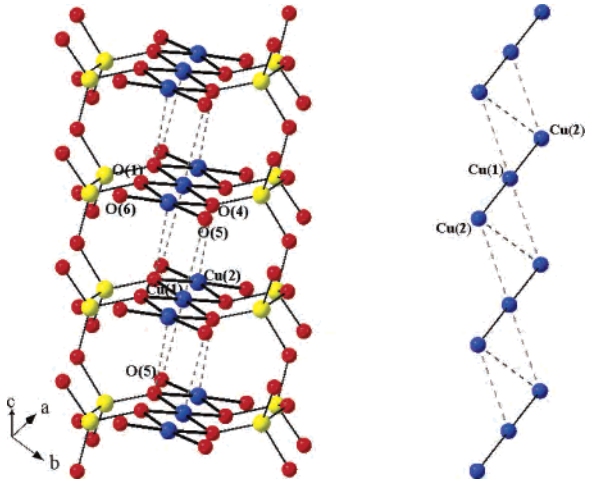

Figure 2. Partial structure of **2** showing (left) the ladderlike lattice made of $[Cu_3O_8]^{10-}$ trimers (rungs) interconnected by $[GeO_3]_\infty$ metagermanate chains (rails) and (right) the arrangement of Cu^{2+} magnetic cations. The dotted lines represent long Cu−O bonds, while the dashed lines indicate weak magnetic interactions via these long bonds (see the text).

containing interwoven $[Cu_3O_9]_\infty^{12-}$ and $[SiO_3]_\infty^{2-}$ metasilicate chains was previously reported.[11]

The most prominent structural feature of this series lies in the ladderlike arrangement of periodic arrays of $[Cu_3O_8]^{10-}$. These trimers are embedded in an extended lattice exhibiting a pseudo-one-dimensional channel framework. The electropositive cations, Li^+ and Na^+, reside in channels constructed by six corner-sharing polyhedral units ($2 \times CuO_4$ and $4 \times GeO_4$), as shown in Figure 1. The $[Cu_3O_8]^{10-}$ trimers are constructed by three square-planar CuO_4 units sharing trans edges in a linear fashion, which is indicated by the nearly 180° dihedral angles. The trimeric nanostructures are stacked along [001] [see Figure 2 (left)], and each shares its vertex O atoms with six $[GeO_3]_\infty$ metagermanate chains facilitating lattice propagation along the *ab* plane.

In **2**, the intratrimer Cu−O bond distances are between 1.92 and 1.98 Å, which are comparable with 1.95 Å, the sum of the Shannon crystal radii for the four-coordinate Cu^{2+} (0.71 Å) and O^{2-} (1.24 Å).[12] The edge-shared CuO_4 units lead to relatively small Cu(1)−O(1)^b−Cu(2) and Cu(1)−O(4)^b−Cu(2) bridging angles of 102.2(1)° and 100.0(2)°, respectively, and a short Cu−Cu distance of 3.03 Å across the shared edge.

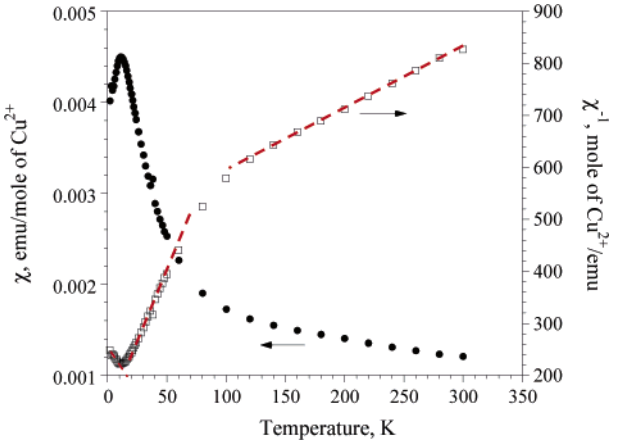

Figure 3. Temperature-dependent magnetic susceptibility χ and inverse magnetic susceptibility χ^{-1} of $Na_2Cu_3Ge_4O_{12}$ taken at a field of 100 G. Three linear regions of the χ^{-1} vs T curve are outlined by red dashed lines (see the text).

The $[Cu_3O_8]^{10-}$ intertrimers are coupled through apical O atoms, giving substantially long Cu−O distances and near 90° Cu−O−Cu bond angles. Along the stacking direction, each center Cu has two long Cu(1)−O(5)^t bonds [2.694(4) Å] through the terminal O atoms of neighboring trimers, as indicated by the dotted lines. Similarly, the two side Cu atoms each have one long Cu(2)−O(4)^b bond [2.553(5) Å] through the bridging O atoms of the neighboring trimeric unit. The intercluster Cu(1)−Cu(2) and Cu(2)−Cu(2) distances (dashed lines) are 3.349(1) and 3.273(1) Å, respectively, and ∠Cu(1)−O(5)−Cu(2), ∠Cu(1)−O(4)−Cu(2), and ∠Cu(2)−O(4)−Cu(2) are between 91.4 and 94.6°.

Judging from the bond distances and angles with respect to the Cu−O framework (Table S2 in the Supporting Information), three possible exchange pathways can be discerned, as highlighted by an isosceles triangle made of one intratrimeric and two intertrimeric couplings in Figure 2 (right). This exchange network may exhibit both frustration and topological ferrimagnetism.[13]

The preliminary analysis of magnetic data suggests that spin interactions in this family of compounds are predominantly antiferromagnetic (AFM), which is attributed to intratrimer spin coupling.[14] Figure 3 shows the temperature-dependent (2−300 K) magnetic susceptibility χ and inverse magnetic susceptibility χ^{-1} of $Na_2Cu_3Ge_4O_{12}$ taken in a small

(11) Kawamura, K.; Kawahara, A. *Acta Crystallogr.* **1976**, *B32*, 2419−2422.

(12) Shannon, R. D. *Acta Crystallogr*, **1976**, *A32*, 751−767.

(13) (a) Greedan, J. E. *J. Mater. Chem*, **2001**, *11*, 37−53 and references cited therein. (b) George, R.; Borras-Almenar, J. J.; Coronado, E.; Curely, J.; Drillon, M. In *Magnetism: Molecules to Materials*; Miller, J. S., Drillon, M., Eds.; Wiley-VCH: Weinheim, Germany, 2001; pp 1−47.

(14) The magnetic susceptibility was measured with a Quantum Design SQUID MPMS-5S magnetometer. Selected single crystals were ground and placed in a gel capsule sample holder. The magnetic susceptibility was corrected for the gel capsule and core diamagnetism with Pascal's constants.

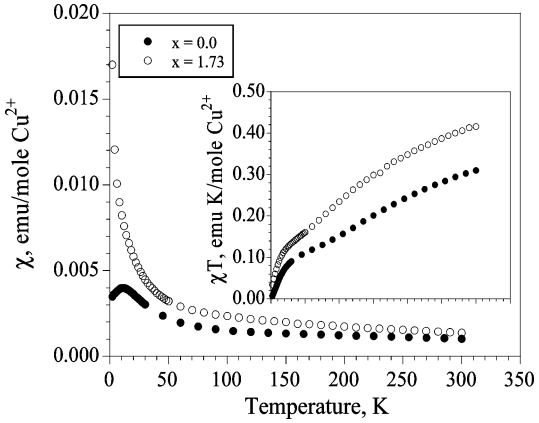

Figure 4. Temperature-dependent magnetic susceptibilities χ and χT (inset) of $Na_2Cu_3Ge_{4-x}Si_xO_{12}$ ($x = 0$ and 1.72) taken at a field of 0.5 T.

applied field ($H = 100$ G). The χ^{-1} vs T plot discloses, to a good approximation, three linear regions (outlined in red dashed lines) that are separated by a broad crossover range. The Curie−Weiss (C−W) fit using $\chi = C/(T - \theta)$ in the temperature range 120 K $\leq T \leq$ 300 K results in a rather large effective magnetic moment, $\mu_{eff} = 2.6(3)\ \mu_{BM}$ per Cu^{2+} ion (as opposed to 1.73 μ_{BM} of the spin-only value) and very negative $\theta = -404(7)$ K. Sighting along the χ^{-1} vs T curve, one can capture the discontinuity of the slope occurring at ca. 100 K, followed by a broad transition before the second AFM region starts at ca. 50 K. The linear fit of the $\chi^{-1}(T)$ vs T curve in the lower temperature range over 26−50 K results in a much less negative Weiss constant $\theta = -25(2)$ K and a reduced Curie constant (by a factor of close to 4.5) and, in turn, calculated $\mu_{eff} = 1.2(2)\ \mu_B$. The trend is pointing toward the possible existence of additional intertrimer ferromagnetic (FM) interactions.

Additional magnetic studies clearly show the expected field dependence of magnetic susceptibilities. In an increased magnetic field ($H = 0.5$ T), μ_{eff} is suppressed and the Weiss constant θ becomes less negative. Compared to **2**, the same C−W fit in the temperature range 110 K $\leq T \leq$ 300 K results in a smaller $\mu_{eff} = 2.3(2)\ \mu_{BM}$ and decreased $\theta = -353(5)$ K. The curve-fit values over the temperature range 25−60 K also vary correspondingly, i.e., 1.17(8) μ_{BM} and −26.5(3) K, respectively.

Additional evidence showing weak intertrimer magnetic interactions lies in the cell volume dependence of magnetic susceptibility upon Si doping. For comparison, Figure 4 shows the χ and χT (inset) vs T plots of the $x = 0$ and 1.72 phases taken at $H = 0.5$ T. The latter shows a comparable $\mu_{eff} = 2.4(2)\ \mu_{BM}$, according to the C−W fit of the χ^{-1} vs T curve over the same temperature range, but significantly increased $\theta = -196(3)$ K. As expected, the fit over $T =$ 8−42 K results in $\mu_{eff} = 1.27(9)\ \mu_{BM}$ and $\theta = -14.4(2)$ K.

It is noted that the large negative θ value at high temperatures is consistent with what is expected according to the Goodenough−Kanamori−Anderson rule,[15] where edge-shared CuO_4 chains usually result in a relatively large AFM coupling if ∠Cu−O^b−Cu is larger than 90°. The less-negative trend upon Si doping suggests a contribution due to the above-mentioned ferrimagnetism.

Further analysis indicates that the bulk magnetic susceptibility could be attributed to the combination of predominantly intratrimer AFM coupling and weak intertrimer FM interaction. It is evident that, below 20 K, the existing FM component dominates. It overcomes the decrease in the magnetic moment, as shown by the upturn of the χ vs T curve observed in the Si-doped sample (Figure 4). The inset also shows an increase in the χT value over the entire temperature range, suggesting a possible intertrimer spin coupling, which increases as the cell volume decreases. The latter could be attributed to geometrically frustrated magnetic coupling via μ_3-O(4) (Figure 2). The overall FM contribution, nevertheless, is weak because of the corresponding long intertrimeric Cu(2)−O(4) distances. The narrowed intertrimer bridging angles upon Si doping (Table S3 in the Supporting Information) could account for an increased FM interaction. Subsequently, the $x = 1.72$ phase, unlike **2**, gives a nonzero χT interception at 0 K, e.g., 0.42 μ_{BM} per Cu^{2+} ion. In fact, we do observe a small departure of susceptibility data measured in zero field cooling (ZFC) from that in field cooling (FC) (Figure S5 in the Supporting Information) on the polycrystalline sample.

As a final remark, this new series of cuprates possesses a rich magnetic phase diagram, and detailed investigations are underway to address the origin of otherwise exotic magnetic ground states. Nevertheless, the title compounds offer an ideal system that consists of nearly molecule-like nanostructures for structure and property correlation studies of magnetic importance. We have demonstrated that, through cation substitution, the geometrically induced magnetic couplings are systematically tunable upon variation of internal chemical bonding.

Acknowledgment. Financial support for this research (Grants DMR-0077321 and -0322905) and the purchase of single-crystal X-ray (Grant CHE-9808165) and X-ray (Grants ESR-9108772, CHE-9207230, and 9808165) diffractometers from the National Science Foundation are gratefully acknowledged.

Supporting Information Available: X-ray crystallographic file, in CIF format, tables of crystallographic data and of selected bond distances and angles, plots of volume vs x, structures showing embedded Cu−O trimers in isomorphous $A_2Cu_3X_4O_{12}$ phases, χT vs T at 100 G (including ZFC/FC) vs 0.5 T for **2** and, UV−vis spectra for **2**. This material is available free of charge via the Internet at http://pubs.acs.org.

IC060292Q

(15) (a) Goodenough, J. B. *Phys. Rev.* **1955**, *100*, 564−573. (b) Kanamori, J. *J. Phys. Chem. Solids* **1959**, *10*, 87−98. (c) Anderson, P. W. In *Solid State Physics: Advances in Research Applications*; Seitz, F., Turnnbull, D., Eds.; Academic: New York, 1963; Vol. 14, pp 99−214.